



FOLFIRINOX Pharmacodynamic Interactions in 2D and 3D Pancreatic Cancer Cell Cultures

Taylor J. Allen-Coyle^{1,2} · Jin Niu³ · Eva Welsch¹ · Neil T. Conlon¹ · Weylon Garner³ · Martin Clynes^{1,2,4} · Finbarr O'Sullivan^{1,2} · Robert M. Straubinger^{3,5} · Donald E. Mager^{3,6} · Sandra Roche¹

Received: 16 June 2022 / Accepted: 2 September 2022 / Published online: 13 October 2022
© The Author(s) 2022

Abstract

The multi-drug combination regime, FOLFIRINOX, is a standard of care chemotherapeutic therapy for pancreatic cancer patients. However, systematic evaluation of potential pharmacodynamic interactions among multi-drug therapy has not been reported previously. Here, pharmacodynamic interactions of the FOLFIRINOX agents (5-fluorouracil (5-FU), oxaliplatin (Oxa) and SN-38, the active metabolite of irinotecan) were assessed across a panel of primary and established pancreatic cancer cells. Inhibition of cell proliferation was quantified for each drug, alone and in combination, to obtain quantitative, drug-specific interaction parameters and assess the nature of drug interactions. The experimental data were analysed assuming Bliss independent interactions, and nonlinear regression model fitting was conducted in SAS. Estimates of the drug interaction term, ψ (ψ), revealed that the Oxa/SN-38 combination appeared synergistic in PANC-1 ($\psi = 0.6$, 95% CI = 0.4, 0.9) and modestly synergistic, close to additive, in MIAPaCa-2 ($\psi = 0.8$, 95% CI = 0.6, 1.0) in 2D assays. The triple combination was strongly synergistic in MIAPaCa-2 ($\psi = 0.2$, 95% CI = 0.1, 0.3) and modestly synergistic/borderline additive in PANC-1 2D ($\psi = 0.8$, 95% CI = 0.6, 1.0). The triple combination showed antagonistic interactions in the primary PIN-127 and 3D PANC-1 model ($\psi > 1$). Quantitative pharmacodynamic interactions have not been described for the FOLFIRINOX regimen; this analysis suggests a complex interplay among the three chemotherapeutic agents. Extension of this pharmacodynamic analysis approach to clinical/translational studies of the FOLFIRINOX combination could reveal additional pharmacodynamic interactions and guide further refinement of this regimen to achieve optimal clinical responses.

Keywords FOLFIRINOX · pancreatic cancer · pharmacodynamic modelling

Introduction

Pancreatic adenocarcinoma (PDAC) has one of the highest mortality rates, with a 5-year survival rate of approximately 9% and an average survival time of less than 6 months (1). The poor prognosis of PDAC is due to a combination of factors including frequent diagnosis at a late stage, when it is locally advanced or metastatic, and its asymptomatic progression (2). Because of the combined effect of genetic and epigenetic modifications in pancreatic tumours, they exhibit an aggressive nature, with therapeutic resistance from an early stage (3, 4).

Surgery remains the only curative option for pancreatic cancer patients; however, less than one in five patients are eligible for surgery. Patients often receive neoadjuvant therapy to down-stage tumour burden and allow resection (5). There is limited data on regimen selection, with the most common therapeutic regimes selected for the metastatic disease being

✉ Taylor J. Allen-Coyle
taylorjade.allencoyle2@mail.dcu.ie

¹ SSPC, The SFI Research Centre for Pharmaceuticals, Limerick, Ireland
² National Institute for Cellular Biotechnology, Dublin City University, Dublin, Ireland
³ Department of Pharmaceutical Sciences, University at Buffalo, State University of New York, New York, Albany, USA
⁴ Pancreatic Cancer Research Fund UK (PCRF), London, UK
⁵ Departments of Pharmacology & Therapeutics, and Cell Stress Biology, Roswell Park Comprehensive Cancer Center, Buffalo, New York, USA
⁶ Enhanced Pharmacodynamics, LLC, Buffalo, New York, USA

FOLFIRINOX (5-fluorouracil (5-FU)/leucovorin (LV), irinotecan and oxaliplatin (6)) or gemcitabine/nab-paclitaxel. There is even less guidance in relation to second-line regimens. Studies comparing the efficacy of FOLFIRINOX versus gemcitabine/nab-paclitaxel are also confounded based on comparisons of different patient populations (7). FOLFIRINOX is the preferred first-line option for patients with metastatic PDAC younger than 76 years and who have good performance status (ECOG 0 or 1). To increase tolerability and decrease side effects, modified FOLFIRINOX regimens typically eliminate the 5-FU bolus loading dose (8, 9). Patients also receive these agents as adjuvant (10) and palliative treatment settings (11, 12).

Empirical clinical optimisation of multi-drug treatment regimens is often hampered by a lack of understanding of pharmacodynamic (PD) drug-drug interactions (DDIs) (13). DDIs can be additive, synergistic or antagonistic (14). With additive interactions, the overall effect of a drug combination is the sum of the pharmacological effects of the individual agents (15). Synergistic interactions have an overall effect that is greater than additive, and conversely, antagonism represents an overall response that is less than additive. However, the approaches to evaluate PD DDIs vary, and these terms are frequently misused (13). PD DDI studies require the assessment of interactions between multiple concentrations of each single agent in the combination, which decreases the feasibility of studying PD interactions in animal models and clinical trials. With the clinical proliferation of combination therapies, there is an increasing opportunity for the application of mathematical modelling strategies to evaluate therapeutic combination regimens (16), which could ultimately enable therapeutic optimisation by modelling and simulation. Improvements in high-throughput experimental and computational techniques are contributing to the growing rationale for using PD DDI modelling in clinical trials (17).

In vitro cellular models of PDAC often fail to represent the heterogeneity of the tumour and the tumour microenvironment. In recent years, a shift to 3D spheroid or organoid models to recapitulate more physiologically relevant morphologies has occurred. Nelson et al. described a method for the establishment of organoids and isogenetically matched 2D primary cell lines from PDAC patient-derived xenograft (PDX) tumour samples (including PIN-127) and recapitulation of the cell lines to cell-line organoids that were shown to be morphologically, molecularly and transcriptionally similar to their PDX-derived tumour organoids (18). Another study compared a large drug panel across 2D and 3D cultures, finding that most cytotoxic agents were less active in 3D, but a few drugs showed greater cytotoxicity in 3D models compared to 2D culture, which proved to be both cell and drug dependent (19). Ait-Oudhia et al. described a 3D and dynamic cellular system suitable for *in*

vitro pharmacokinetic (PK) and PD analysis of combination therapies and compared this to static 2D culture, showing that 2D data successfully predicted the 3D data profiles (20). These studies highlight the importance of incorporating multiple cellular models into drug screening experiments.

Here, we investigated PD DDIs of the drugs in the FOLFIRINOX regimen to determine the nature of their interactions, using both primary and established pancreatic cancer cell lines cultured as 2-D and 3-D models. The three cytotoxic agents of FOLFIRINOX were evaluated alone, in pairwise combinations, and together over ranges of concentrations. For each combination, a quantitative DDI term, ψ (ψ), was derived to express the nature and magnitude of the interaction. Established pharmacodynamic modelling strategies for pairwise comparisons of drug interactions were extended to include triple drug combinations.

Materials and Methods

Cell Culture

The human pancreatic cell-line MIAPaCa-2 was obtained from the European Collection of Cell Cultures (ECACC, UK). BxPC-3 and PANC-1 human pancreatic cancer cell lines were obtained from the American Type Culture Collection (ATCC, Rockville, MD, USA). PIN-127 cells were derived in-house from a patient-derived xenograft model as previously described (21).

PANC-1 and MIAPaCa-2 cells were grown in DMEM (Sigma-Aldrich, Dublin, Ireland) supplemented with 5% (v/v) fetal bovine serum (FBS) (Thermo Fischer Scientific, UK) and 2% L-glutamine. BxPC-3 cells were grown in RPMI-1640 medium supplemented with 5% (v/v) FBS. PIN-127 cells were cultured in DMEM/F-12 Hams medium supplemented with 10% (v/v) FBS (Corning, SA). Cells were grown in a humidified atmosphere with 5% CO₂ at 37°C in culture flasks. Cells were sub-cultured, using PBS to wash and trypsin-EDTA (Bio-Sciences Ltd, Ireland) to detach when cells reached 80–90% confluency.

Reagents

SN-38, the active metabolite of irinotecan, was obtained from Stratech Scientific Ltd (Ely UK). A 10 mM SN-38 stock solution was prepared in DMSO and stored as aliquots at –20°C. Leucovorin was purchased from Sigma-Aldrich (Dublin, Ireland), and 10 mM stocks were prepared in water. 5-Fluorouracil (5-FU) and oxaliplatin (Oxa) were supplied as clinical formulations from St. Vincent's University Hospital, Dublin, at stock concentrations of 192 mM and 12.5 mM, respectively, and stored at room temperature. All

reagent aliquots were dated upon reconstitution and assessed to ensure efficiency was consistent between replicates.

2D Proliferation Assay

MIA-PaCa-2, PANC-1, BxPC-3 and PIN-127 cells were seeded in 96-well plates at a density of 1 cells/mL, 2 cells/mL, 3 cells/mL, and 5×10^4 cells/mL, respectively, and incubated overnight at 5% CO₂ and 37°C. The following day, freshly prepared drug dilutions were added to each well. Two approaches were taken for drug exposure concentrations. (1) **Fixed ratio**: cells were treated with single, pairwise and triple combinations at a fixed ratio, or (2) **Varying ratio**: pairwise drug combinations at 5 concentrations of each drug, resulting in 25 combinations were tested. The plates were incubated for a further 6 days until control cells approached confluency. Following incubation with the drug, the media was removed, and cell proliferation was quantified using an acid phosphate assay as previously described (22). Briefly, the wells were washed with phosphate-buffered saline (PBS). Paranitrophenol phosphate (PNP) (ThermoFisher) substrate (10 mM PNP in sodium acetate buffer, pH 5.5) was added to each well and incubated (37°C) for 1–2 h; 50 µL 1 M NaOH was added, and the absorbance was read at 405 nm (reference – 620 nm).

Both methods required different analysis software. Schema (1) in which cells were treated with single, pairwise and triple combinations at fixed ratio were analysed using SAS 9.4 software as described in the ‘[Mathematical Modelling](#)’ section. Schema (2) in which cells were treated with varying ratios of pairwise combinations at 5 concentrations of each drug was analysed using Combenefit™, as described in the ‘[Analysis of Varying Pairwise Ranges Using Combenefit™ Software](#)’ section.

Analysis of Varying Pairwise Ranges Using Combenefit™ Software

As described in the ‘[2D proliferation assay](#)’ section, BxPC-3 and PIN-127 cells were examined using a varying pairwise concentration proliferation assay. *In vitro* experimental data were analysed using a surface approach, in which data were compared to mathematical models of concentration response for additive combinations. To keep results comparable, the Bliss model was selected. In brief, an experimental concentration–response surface that describes the combination effect in a concentration space was derived from a matrix of percentage of control values across concentrations. The effect of the single agents was extracted from the data by curve fitting. Based on the single agent curves, a model-based pairwise combination concentration–response surface was composed, providing a ‘reference’ surface for additivity.

Experimental and model-generated combination concentration–response surfaces were then compared, resulting in a synergy distribution in concentration space (23).

3D Cell Proliferation Assay

96 well plates coated with 50 µL polyhema (Sigma-Aldrich S3932, 5 mg/mL in 96% ethanol) were baked at 50°C for two days. Plates were stored at room temperature for up to 6 months. PANC-1 cells (90 µL/well) were seeded at 2×10^4 cells/mL in 5% FBS DMEM with Matrigel™ (Sigma-Aldrich) (2%) and incubated overnight at 37°C. Serial drug dilutions in complete media (30 µL) or drug-free media (control) were added to the wells and incubated at 37°C. After 9 days, cells were quantified using alamarBlue® Cell Viability assay (Invitrogen) to avoid the washing steps required for the acid phosphate assay. Briefly, 12 µL of alamarBlue® reagent (10% of final volume) was added to the wells and incubated at 37°C for 4 h, and fluorescence was measured at 535/590 nm excitation/emission wavelength on a Biotek plate reader using KC4 software. The blank for the background consisted of media and 2% Matrigel™. Percent viability was calculated relative to untreated control. Each assay was performed in biological triplicate.

Mathematical Modelling

Single-drug Studies

For single-agent 5-FU, oxaliplatin and SN-38, the IC₅₀ (half maximal inhibitory concentration) values were determined using the Hill equation (Table I, Eq. (1)). In this equation, R_i represents the viability of cells after 5 days of exposure to drug i ; I_{\max} represents the maximum inhibition achieved at a high concentration; C represents the concentration used for testing; IC_{50} represents the concentration to achieve 50% of I_{\max} ; and m is the Hill coefficient that corresponds with the steepness of the inhibition curve. These parameters provided the foundation for further pairwise and triple drug combination studies and associated modelling. The data were analysed by nonlinear regression to provide a statistical analysis of the estimated parameters.

Pairwise Drug Combinations

A universal response surface approach to fit all data simultaneously was applied to the Bliss independent model to analyse cell viability data for PANC-1 (2D and 3D), MIA-PaCa-2, BxPC-3 and PIN-127 (24, 25). In Eq. (2) (Table I), i and j represent the two drugs in a combination pair; and ψ (ψ) is the drug interaction term for combination treatments. The interaction term ψ is introduced into the equation to quantify interaction in combination groups. If $\psi < 1$, the

Table I Pharmacodynamic Equations for Model Fitting

$R_i = 100\% \cdot \left(1 - I_{max,i} \cdot \frac{C_i^{m_i}}{C_i^{m_i} + IC_{50,i}^{m_i}} \right)$	1
$R = 100\% \cdot \left(1 - I_{max,i} \cdot \frac{C_i^{m_i}}{C_i^{m_i} + IC_{50,i}^{m_i}} \right) \cdot \left(1 - I_{max,j} \cdot \frac{C_j^{m_j}}{C_j^{m_j} + (\psi) \cdot IC_{50,j}^{m_j}} \right)$	2
$R = 100\% \cdot \left(1 - I_{max,i} \cdot \frac{C_i^{m_i}}{C_i^{m_i} + IC_{50,i}^{m_i}} \right) \cdot \left(1 - I_{max,j} \cdot \frac{C_j^{m_j}}{C_j^{m_j} + IC_{50,j}^{m_j}} \right) \cdot \left(1 - I_{max,k} \cdot \frac{C_k^{m_k}}{C_k^{m_k} + (\psi) \cdot IC_{50,k}^{m_k}} \right)$	3

SAS 9.4 software was used to model the effect of the single, pairwise and triple combinations on cell proliferation. The equations were applied to single (Eq. (1)), pairwise (Eq. (2)) and triple (Eq. (3)) combination data to determine pharmacodynamic interactions. I_{max} represents the maximum inhibition achieved at high concentrations. IC_{50} represents the concentration to achieve 50% of I_{max} , and m is the Hill coefficient that corresponds with the steepness of the inhibition curve

interaction is synergistic, additive if $\psi = 1$, and antagonistic if $\psi > 1$. Upper and lower 95% confidence intervals were used to show statistically significant interaction indexes. In fitting the data, ψ was estimated separately for both drugs to evaluate the sensitivity of the calculated value.

Triple Drug Combination

The FOLFIRINOX combination includes leucovorin (LV) as a potential sensitiser of tumour cells to 5-FU (26, 27). *In vitro* analysis of the 5-FU/LV combination showed no significant synergistic effect (Supplementary Fig. S2). Therefore, further analyses included only the three cytotoxic FOLFIRINOX drugs. For pharmacodynamic modelling of the triple drug combination, Eq. (2) was expanded, as shown in Eq. (3) (Table I). In estimating ψ , the fitted value was assigned to the IC_{50} of each cytotoxic agent as follows: 5-FU (MIAPaCa-2/BxPC-3), SN-38 (PANC-1 2D/3D) and 5-FU and Oxa (PIN-127).

Model Fitting

Model fitting was conducted in SAS 9.4 (Cary, NC) using the nonlinear regression procedure ‘nlin’ with the MARQUARDT method (Fig. 1). The models were weighted by the square of the fitted values (i.e. inverse of the variance). The theoretical additive responses were calculated by Monte-Carlo simulation considering the uncertainty of parameter estimation and random experimental error [28].

Results

Effect of the Single FOLFIRINOX Agents in Pancreatic Cancer Cells

Concentration-effect assays of each single agent were performed to determine IC_{50} values. The 2D assays employed

an acid phosphatase end-point assay, whereas the 3D assays employed alamarBlue to estimate cell proliferation. alamarBlue measures cellular metabolic activity; the active ingredient resazurin is reduced to the resorufin product within viable cells and as such is an indirect measure of cell proliferation. To ensure comparability, a comparison of the alamarBlue and acid phosphatase proliferation assays was performed for the triple combination in PANC-1 cells, and the results were statistically equivalent (Supplementary Fig. S1).

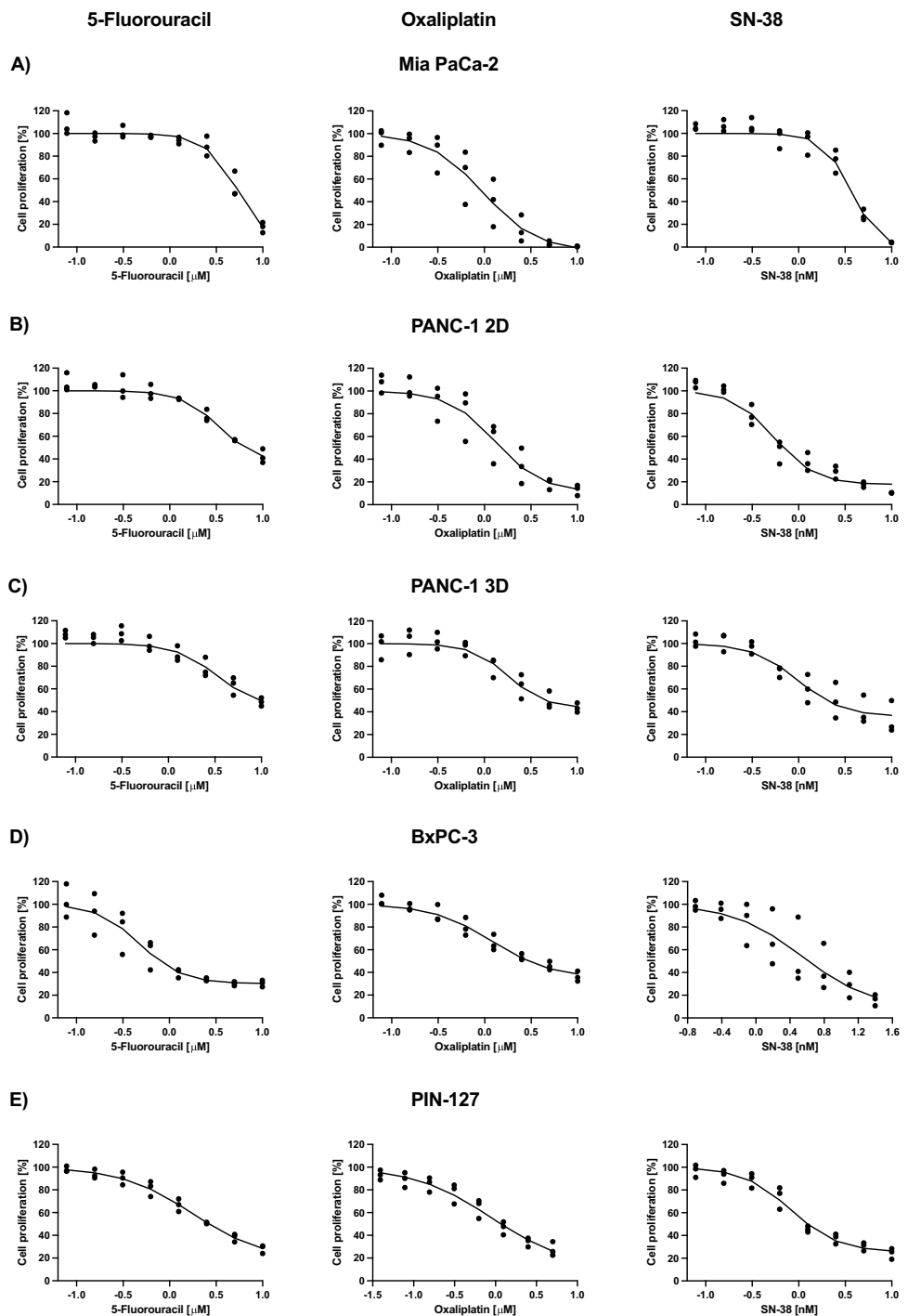
Model-estimated parameters I_{max} , IC_{50} and m (Table II) were consistent with the experimental data in Fig. 1. Varying responses to each single agent were observed for each cell line (Table II). BxPC-3 cells were the most sensitive to 5-FU ($IC_{50} = 0.5 \mu\text{M}$), and MIAPaCa-2 cells were the least sensitive ($IC_{50} = 5.4 \mu\text{M}$). The primary cell-line PIN-127 was the most sensitive to oxaliplatin and to SN-38. PANC-1 cells were the least sensitive to SN-38 in these *in vitro* studies in both 2D ($IC_{50} = 7.6 \text{ nM}$) and 3D ($IC_{50} = 42.9 \text{ nM}$) cultures.

Leucovorin (LV), a potentiator of 5-FU efficacy (26), was tested alone and combined with 5-FU across the panel of cell lines. Supplementary Fig. S2 shows that single-agent LV had no effect on cell proliferation and no statistically significant potentiating effect in combination with 5-FU. Therefore, the remaining evaluation of 2- and 3-drug effects on the cell-line panel included only the 3 cytotoxic agents of the FOLFIRINOX combination.

Combination of Oxaliplatin and SN-38 Synergistically Inhibits Cell Proliferation Across Multiple Pancreatic Cancer Cell Lines

Analysis of the pairwise pharmacodynamic interactions of each agent of the FOLFIRINOX regimen demonstrated that oxaliplatin and SN-38 was the only combination that showed synergistic interactions across two cell lines. This synergy was observed in MIAPaCa-2 (2D) and PANC-1 (2D), as shown in Table III. This suggests that oxaliplatin

Fig. 1 Experimental versus model-fitted responses. SAS 9.4 software was used for nonlinear regression to generate the model-fitted values for the single-drug experiments in all cell lines. The points on the graphs represent the observed data, and the solid sigmoidal lines represent the model-fitted curves. Columns 1–3 represent 5-FU, oxaliplatin and SN-38. Cell lines are separated into rows A–E: MIAPaCa-2 (A), PANC-1 2D (B), PANC-1 3D (C), BxPC-3 (D) and PIN-127 (E)



and SN-38 were the most potent pairwise combination. Borderline additive interactions were observed between 5-FU and oxaliplatin in the MIAPaCa-2 cell line, whereas interactions trending towards antagonism were observed across all other cell lines. SN-38 and 5-FU interactions were additive in both the MIAPaCa-2 and PANC-1 cell lines but trended towards antagonistic in the PIN-127, BxPC-3 and PANC-1 3D cells, with ψ values ranging from 1 to 8.4 (Table III). These results suggest that 5-FU/Oxa and SN-38/5-FU show

less beneficial DDI than oxaliplatin/SN-38 in this panel of pancreatic cancer cells.

Each of the pairwise drug combinations displayed antagonistic interactions in the primary PIN-127 and KRAS wild-type BxPC-3 cell lines, with ψ values listed in Table III. To evaluate these drug interactions further, BxPC-3 (Fig. 2) and PIN-127 (Fig. 3) cell proliferation was evaluated in a 5×5 grid of concentrations. Experimental response to these varying concentrations as percentage proliferation compared to

Table II Model-estimated Pharmacodynamic Parameters for the Single Agent Chemosensitivity Experiments Across All Cell Lines

Cell line	Drug	I _{max}	SE	IC ₅₀	SE	m	SE
PIN-127	5-FU	0.8	0.1	1.8	0.3	1.1	0.2
	Oxal	0.9	0.1	0.9	0.3	0.9	0.1
	SN38	0.7	0.0	1.7	0.0	1.7	0.2
BxPC-3	5-FU	0.7	0.0	0.5	0.1	1.9	0.5
	Oxal	0.6	0.1	1.2	0.4	1.4	0.4
	SN38	0.9	0.1	5.1	0.0	1.1	0.3
MIA PaCa-2	5-FU	1.0	0.2	5.4	1.2	2.4	0.7
	Oxal	1.0	0.1	1.0	0.1	1.5	0.2
	SN38	1.0	0.1	1.8	0.0	2.8	0.5
PANC-1 (2D)	5-FU	0.6	0.1	3.4	0.8	2.1	0.7
	Oxal	0.9	0.0	1.3	0.2	1.7	0.3
	SN38	0.8	0.0	7.6	0.0	2.0	0.3
PANC-1 (3D)	5-FU	0.6	0.1	3.3	1.1	1.9	0.7
	Oxal	0.6	0.1	1.8	0.3	2.2	0.6
	SN38	0.6	0.0	42.9	0.0	1.8	0.4

Parameter values were derived by nonlinear regression using SAS 9.4, and parameter abbreviations are defined in Table I
MG, model generated; SE, standard error

Table III Summary of the Pairwise Combinations Across the Cell Lines

Cell line	Pairwise Combination	Psi Value (ψ)	SE	95% CI Lower	95% CI Higher
PIN-127	5-FU + Oxa	3.9	0.9	2.1	5.7
	Oxa + SN-38	4.2	1.5	1.2	7.3
	SN-38 + 5-FU	1.9	0.3	1.2	2.6
BxPC-3	5-FU + Oxa	1.2	0.2	0.8	1.6
	Oxa + SN-38	2.2	1.0	0.1	3.3
	SN-38 + 5-FU	1.7	0.5	0.6	2.7
MiaPaCa-2	5-FU + Oxa	1.0	0.1	0.8	1.2
	Oxa + SN-38	0.8	0.1	0.6	1.0
	SN-38 + 5-FU	1.0	0.0	0.9	1.1
PANC-1 (2D)	5-FU + Oxa	1.3	0.1	1.0	1.6
	Oxa + SN-38	0.6	0.1	0.4	0.9
	SN-38 + 5-FU	1.0	0.1	0.6	1.2
PANC-1 (3D)	5-FU + Oxa	1.1	0.2	0.6	1.6
	Oxa + SN-38	1.0	0.2	0.4	1.5
	SN-38 + 5-FU	8.4	2.3	3.6	13.1

The psi (ψ) interaction term was estimated for the combinations using Eq. (2) (Table I). Interactions were categorised as synergistic ($\psi < 1$), additive ($\psi = 1$) or antagonistic ($\psi > 1$). Red indicates antagonism, orange indicates additivity, and green identifies combinations with synergistic interactions

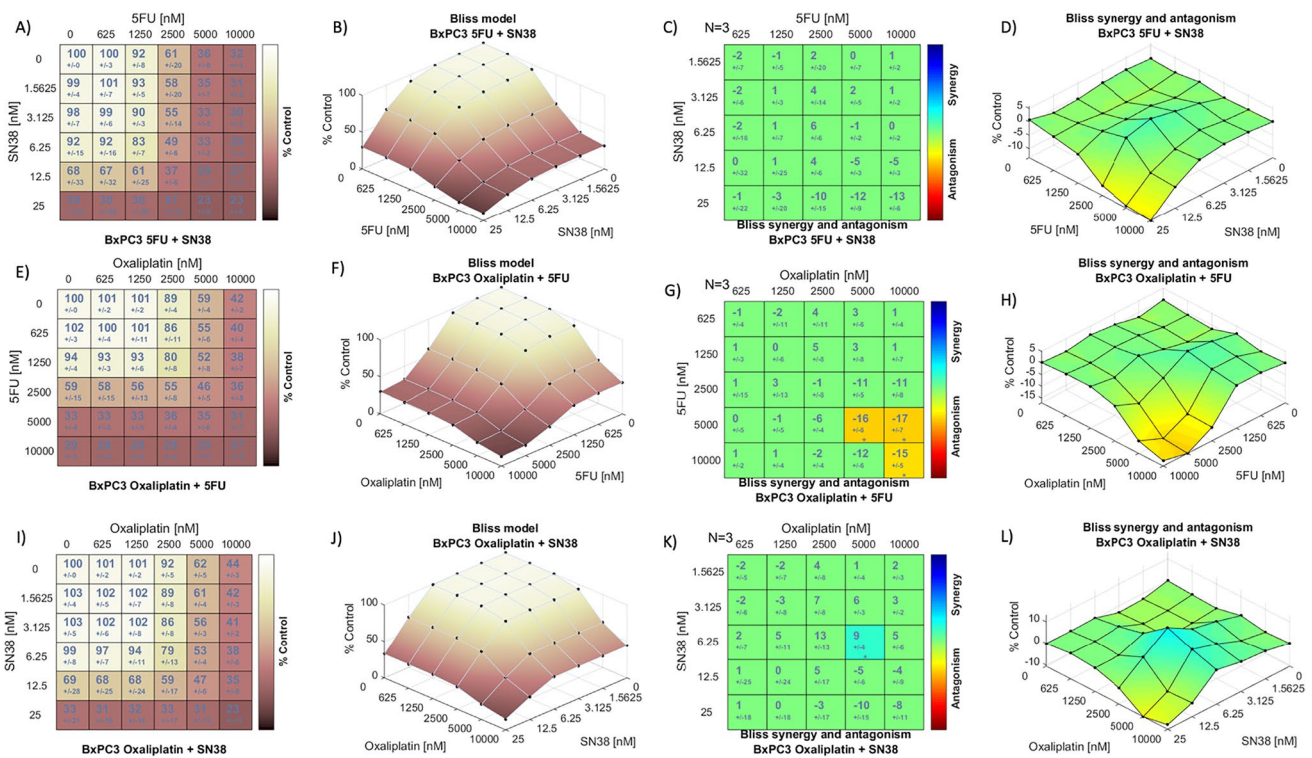


Fig. 2 Pairwise combinations produce varying areas of strong antagonism and synergy in BxPC-3 cells. **A–D**: response to 5-FU/SN-38, **E–H**: response to Oxa/5-FU, **I–L**: response to Oxa/SN-38. Analysis of altering concentration–response represented in matrix format (**A, E, I**) and surface plot (**B, F, J**) as a percentage of proliferation compared to media control. **Synergy levels in matrix format (C, G, K)** represent the synergy/antagonism score with the

standard deviation number listed below; only coloured synergy levels were significant following a one-sample *t*-test ($*p$ -value $< 5 \times 10^{-2}$; $**p$ -value $< 10^{-3}$; $***p$ -value $< 10^{-4}$). This is generated by CombeneFit™ according to the **Bliss independent model** in comparison to the reference concentration–response surface (**D, H, L**). Data, mean \pm SD, $n = 3$

control is shown in Fig. 2A, E, I (BxPC-3) and Fig. 3A, E, I (PIN-127). Bliss scores generated by CombeneFit™ are coloured when greater than 0 to indicate statistically significant synergistic effects. The experimental combination concentration–response surface, with an overlay of synergy levels, illustrated the inhibition of proliferation achieved within the concentration space (Fig. 2B, F, J: BxPC-3 and Fig. 3B, F, J: PIN-127). Figure 2K, L shows an identified area of synergy for BxPC-3 cells, but it was narrowly confined at 5 μ M oxaliplatin and 6.25 nM SN-38. Substantial antagonism was observed for oxaliplatin and 5-FU at higher drug concentrations, with antagonism scores ranging from -15 to -17 , as shown in Fig. 2G, H. Importantly, the overall interactions remained additive or antagonistic in agreement with the model fitting results shown in Table III. This highlights how pharmacodynamic modelling could be used to identify potential opportunities to increase efficacy and minimise overlapping toxicity by utilising lower drug concentrations.

In PIN-127 cells, the combination of 5-FU and SN-38 showed numerous antagonistic combination ratios at the higher concentration range for both drugs (Fig. 3C, D). Antagonism scores ranged from -8 to -17 ; 5-FU (2.5 μ M,

5 μ M, and 10 μ M) combined with SN-38 (5 nM and 10 nM) were antagonistic, with the highest antagonism observed between 5 μ M and 10 μ M 5-FU and 5 nM SN-38. Figure 3G, H displays the antagonism observed between 5 μ M oxaliplatin and 10 μ M 5-FU, with an antagonism score of -9 (p -value < 0.05). At the higher concentration ratios, antagonism was observed for the pairwise combination of oxaliplatin and SN-38; antagonism scores of -14 and -10 were observed at 5 μ M Oxa/5 nM SN-38 and 2.5 μ M Oxa/10 nM SN-38, respectively. These antagonistic interactions are concordant with the findings from fixed-concentration treatment experiments shown in Table III. These trends of antagonism between the pairwise combinations in the BxPC-3 and PIN-127 cell lines were mirrored in the triple combination.

A Range of Antagonistic Interactions Found Among the 3-Drug Combination

MIAPaCa-2 was the most sensitive to the triple combination of 5-FU, oxaliplatin and SN-28, showing strongly synergistic interactions (Table IV). Whereas PANC-1 cells displayed marginally synergistic interactions in

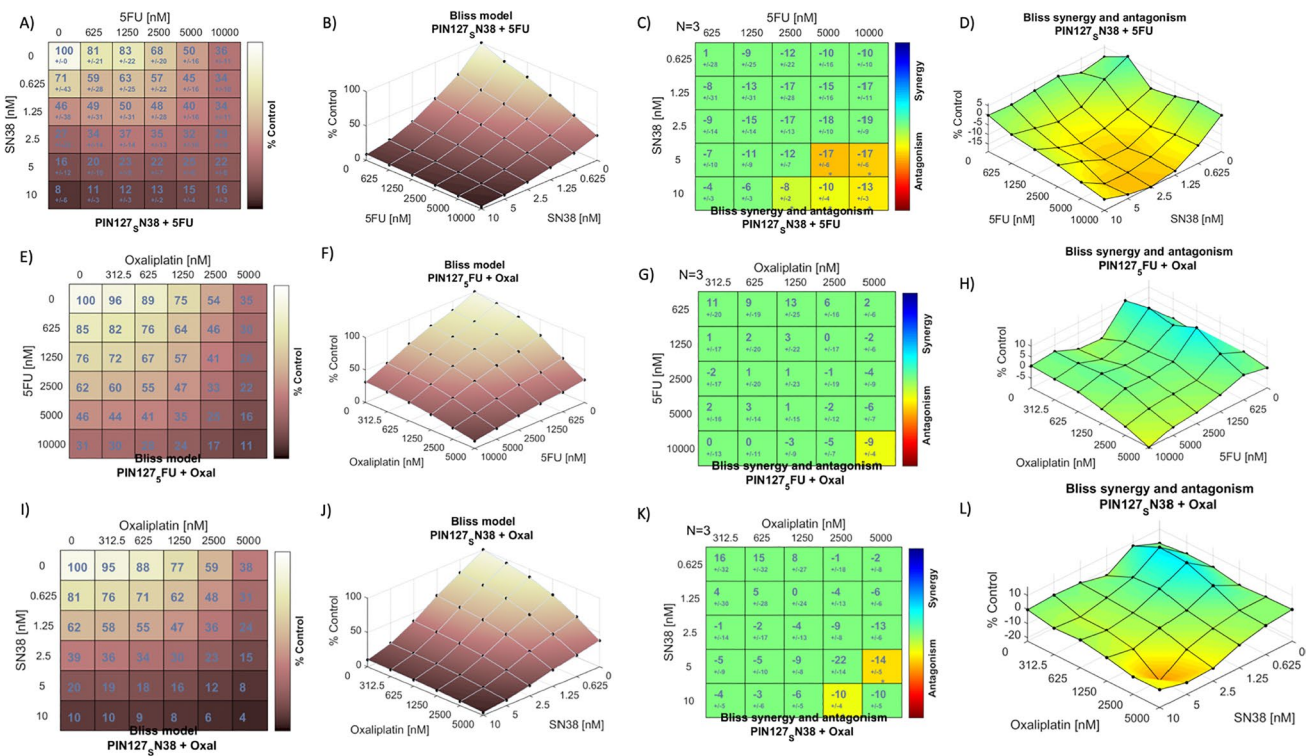


Fig. 3 Pairwise combinations produce areas of strong antagonism in primary PIN-127 pancreatic cancer cells. **A–D**: response to 5-FU/SN-38, **E–H**: response to Oxa/5-FU, **I–L**: response to Oxa/SN-38. Analysis of altering concentration–response represented in matrix format (**A, E, I**) and surface plot (**B, F, J**) as a percentage of proliferation compared to media control. Synergy levels in matrix format (**C, G, K**) represent the synergy/antagonism score with the

standard deviation number listed below; only coloured synergy levels were significant following a one-sample *t*-test (**p*-value < 5 × 10⁻²; ***p*-value < 10⁻³; ****p*-value < 10⁻⁴). This is generated by Combenefit™ according to the Bliss independent model in comparison to the reference concentration–response surface (**D, H, L**). Data, mean ± SD, *n* = 3

Table IV Summary of the Triple Combination Across the Panel of Cell Lines

Cell line	Triple Combination	Psi Value (ψ)	SE	95% CI Lower	95% CI Higher
PIN-127	5-FU + Oxa + SN38	5.6	1.6	2.3	8.8
BxPC-3	5-FU + Oxa + SN38	1.4	2.1	0.4	1.6
Mia PaCa-2	5-FU + Oxa + SN38	0.2	0.05	0.1	0.3
PANC1 (2D)	5-FU + Oxa + SN38	0.8	0.1	0.6	1.0
PANC1 (3D)	5-FU + Oxa + SN38	1.6	0.3	1.0	2.3

The interaction term ψ was estimated in combination treatments using Eq. (3) (Table I). Red indicates antagonism, and green identifies combinations with synergistic interactions

2D, the ψ value changed from 0.8 to 1.6 in 3D conditions, indicating additivity trending towards antagonism. Although synergy/additivity was observed in MIA PaCa-2 and PANC-1, respectively, simultaneous exposure to the triple combination resulted in antagonistic interactions

in the other cell lines (Table IV): PIN-127 ($\psi = 5.6$), BxPC-3 ($\psi = 1.4$) and PANC-1 in 3D ($\psi = 1.6$). Nevertheless, despite indications of antagonism, the triple combination resulted in the greatest overall reduction in cell proliferation compared to each pairwise combination

Fig. 4 Effect of double and triple combination agents. The response was assessed as a % reduction in cell proliferation compared to untreated (y-axis). Combinations tested were 5-FU, Oxa and SN-38 in pairwise vs triple combinations. The x-axis represents drug concentration in μM (5-FU/Oxa) or nM (SN-38). Cell lines are displayed as follows: **A** PANC-1 2D, **B** PANC-1 3D, **C** BxPC-3, **D** PIN-127 and **E** MIAPaCa-2. Data represents the average and standard deviation of three biological replicates

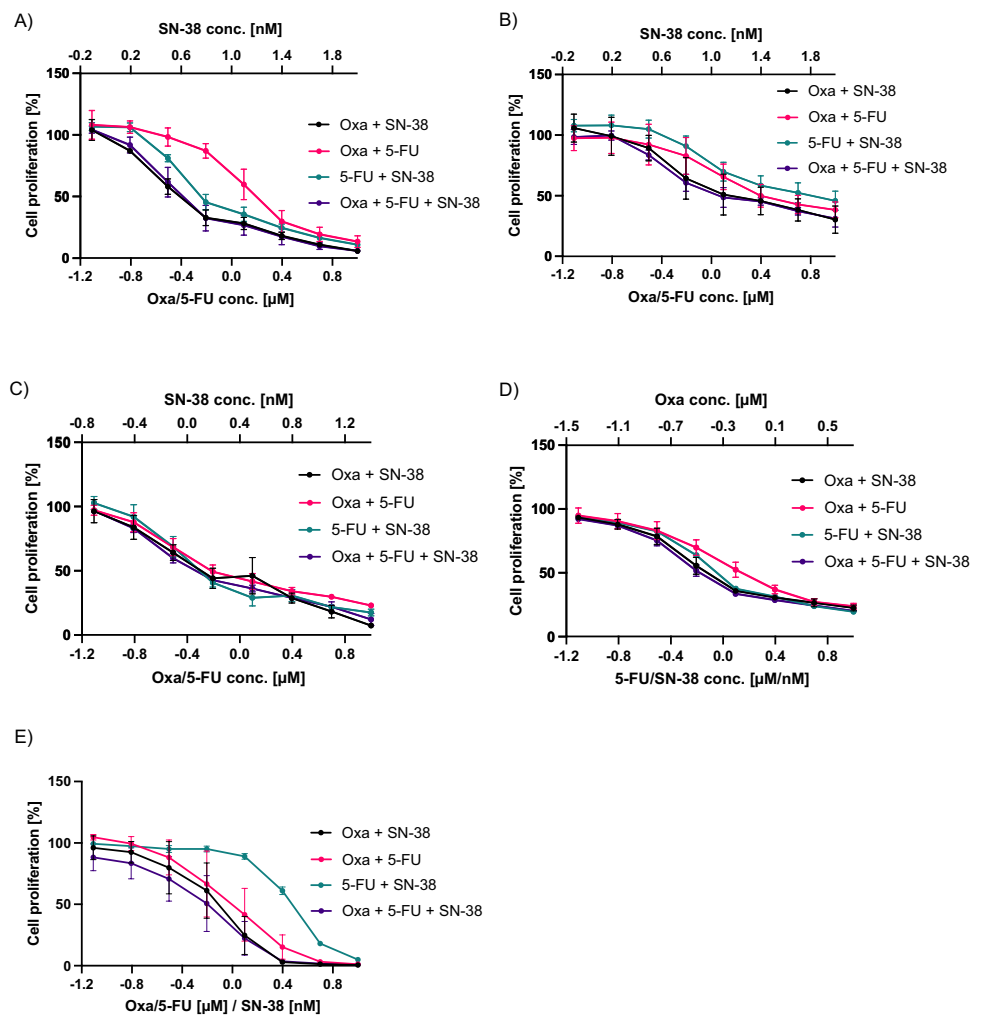


(Fig. 4), except for the BxPC-3 cell line, where oxaliplatin plus SN-38 mediated the greatest reduction in proliferation (Fig. 4C). Oxaliplatin plus SN-38 was also the second-most effective combination at reducing proliferation across the remaining cell lines and was shown to be the only combination demonstrating synergistic interactions.

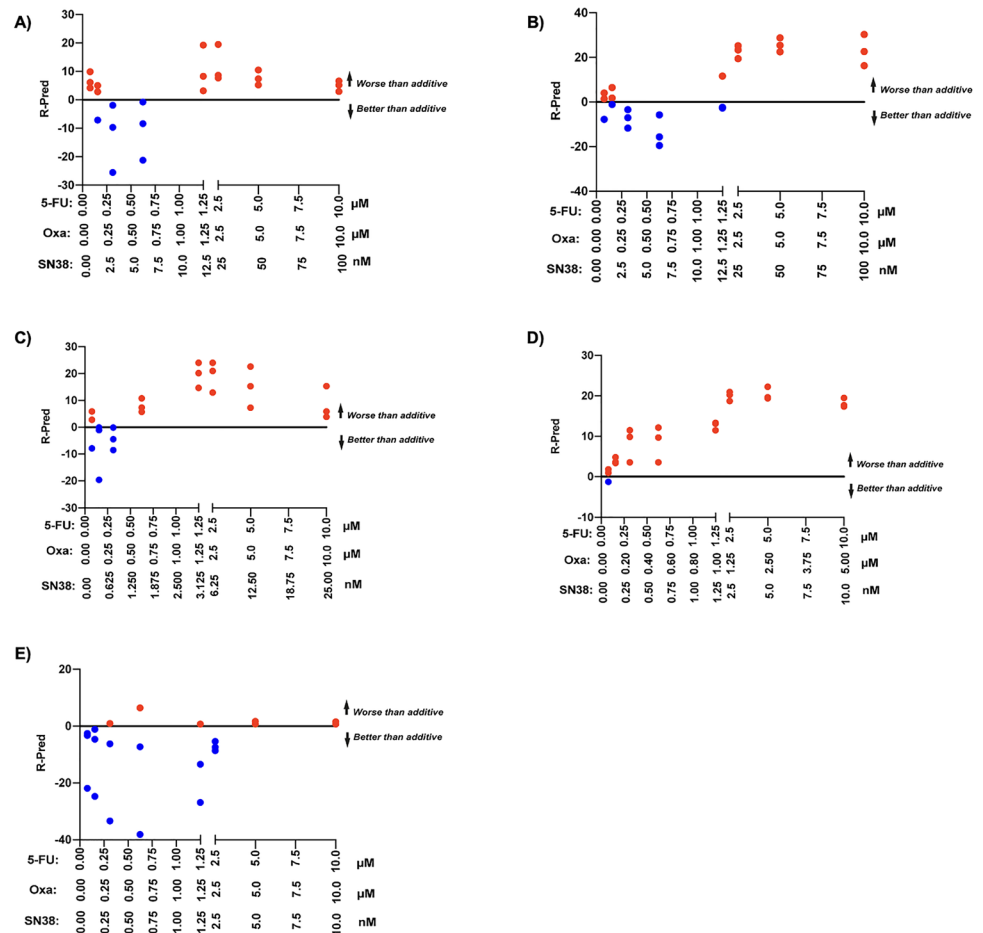
Figure 5 displays the drug interaction score for multiple concentrations combinations of the triple drug combination for each cell line. In agreement with the antagonism of the triple combination, the majority of experimental points displayed in Fig. 5 are above the y-axis horizontal line (model-predicted additivity) and are coloured red symbolising antagonistic interactions. Lower concentrations of the triple combination were better than additive in both PANC-1 2D and 3D cultures (Fig. 5A, B). Figure 5E shows that this combination is strongly synergistic in MIAPaCa-2 cells, as the majority of points are below the y-axis horizontal even at relatively low drug concentrations.

Discussion

Despite the clinical superiority of FOLFIRINOX over gemcitabine as first-line therapy in patients with metastatic pancreatic cancer, the regime is associated with a greater toxicity profile. Patient selection and monitoring is of prime importance (6). The high observed toxicity raised the question as to how the regime could be optimised to increase its availability to more patients. Optimisation of the regime requires a better understanding of the pharmacodynamic drug-drug interactions among the agents of the FOLFIRINOX regimen. In the present study, we investigated the interaction between Oxa, 5-FU and the active metabolite of irinotecan, SN-38, to obtain *in vitro* evidence of potential opportunities for optimising the combination of these chemotherapeutics for the treatment of pancreatic cancer.

As listed in Table II, IC_{50} values for each drug were established for a range of pancreatic cancer cell lines

Fig. 5 Drug interactions among triple combination agents. The X horizontal line (R-Pred) that intercepts $Y=0$ represents predicted additivity (Pred), while all points above or below this line represent the experimental response (R). Each dot represents a biological replicate. All dots above the x horizontal represent drug concentrations which are worse than additive and are coloured red to represent antagonism. All dots below the x represent better than additive and are coloured blue to signify synergistic interactions. Cell lines are represented as follows: **A** PANC-1 2D, **B** PANC-1 3D, **C** BxPC-3, **D** PIN127 and **E** MIAPaCa-2



(MIAPaCa-2, PANC-1 – 2D and 3D, BxPC-3) and primary cells (PIN-127). As single agents, SN-38 was the most potent on all cell lines, with only nm concentrations required for 50% cell growth inhibition. Of the two agents used at μM concentrations, cell lines were most sensitive to Oxa, except for BxPC-3 which was most sensitive to 5-FU. In a panel of human PDAC cell lines similar to those used in this study, Chowbay et al. found that all were most sensitive to single-agent oxaliplatin (29). We found that overall, the PANC-1 cell line was least sensitive to the single agents, with IC_{50} values increasing significantly in 3D cultures. Others have also found increased resistance to chemotherapeutics in PANC-1 cells (29, 30).

Our study found that LV combined with 5-FU had no significant potentiating effect *in vitro* and thus was not carried further into triple combination studies. LV's mechanism of action *in vivo* is the stabilisation of the ternary complex of thymidylate synthase, 5-fluoro-2'-deoxyuridine-5'-monophosphate and the folate cofactor 5,10-methylene tetrahydrofolate (31). LV increases levels of reduced folates in tissues overcoming the short half-life of 5-FU (31, 32). This complex interaction is not replicated in cell culture models that lack contributions of liver catabolism. Others

have found in *in vitro* and *in vivo* experiments that cell lines with high thymidylate synthase expression display greater enhancement of 5FU cytotoxicity by LV (33, 34). Nakamura et al. demonstrated that in cell lines with low expression levels of thymidylate synthase mRNA, LV could not enhance the cytotoxicity of 5FU (35). Furthermore, the enhancement of 5FU cytotoxicity may be saturated by the folic acid content of the cell culture medium and serum because of limited thymidylate synthase expression of the cells investigated. Here, BxPC-3 showed the greatest LV enhancement of 5-FU (Supplementary Fig. S1A). These cells were cultured in RPMI-1640 medium, which has the lowest concentration of folic acid compared to other media: 0.001 g/L.

Oxaliplatin plus SN-38 was the only pairwise combination to show synergistic interactions across multiple cell lines (MIAPaCa-2 and PANC-1 2D; Table III), however, the ψ determined for PANC-1 ($\psi = 0.6$, $\text{CI} = 0.4\text{--}0.9$) was the only interaction where the CI values did not overlap with the additive interaction range. Interestingly, this combination trended towards antagonistic at fixed-concentration combinations in BxPC-3, but demonstrated areas of synergy in a 5×5 concentration grid. For example, high-concentration oxaliplatin with low-concentration SN-38

resulted in a synergy score of 9 (Fig. 2K,L). This suggests that investigating concentration ratios, in combination with pharmacodynamic modelling, can provide valuable insight into multi-drug chemotherapeutic regimens. Previous studies demonstrated that SN-38 and Oxa reciprocally affect the cellular response to DNA damage, resulting in synergy between these drugs (36). A recent study developed polymeric micelles bearing the active forms of irinotecan and Oxa (SN-38/m and DACHPt/m), which showed remarkable cytotoxicity in human pancreatic cancer cell lines (37). Like the current study, their results highlighted the importance of drug ratios to achieve synergy. They found that the clinically used drug weight ratio (irinotecan: Oxa = 2:1) was the least effective for the combination of the active compounds SN-38/m and DACHPt/m. Here, SN-38 was used in nm concentrations at high drug weight ratios for Oxa:SN-38, with the highest ratio (Oxa:SN-38 = 800:1), resulting in synergy in BxPC3 cells. The alteration of drug concentration ratios in the primary PIN-127 cell line did not result in a synergistic shift, but instead brought attention to the antagonistic relationship between the agents in this cell line, particularly at higher concentrations of both drugs (Fig. 3). The PIN-127 cell line was isolated from a PDX model and has previously been shown to harbour KRAS and phosphoinositide-3-kinase regulatory subunit 1 (PI3K31) mutations (21). BxPC3 cell line is a KRAS wild-type cell line (38). Therefore, the KRAS mutation is unlikely to explain the clustering of antagonistic responses observed in these two cell lines.

Oxa and 5-FU pairwise combination was found to be antagonistic in 4 out of 5 cell lines examined. PIN-127 showed strong synergy ($\psi = 3.9$, 95% CI = 2.1, 5.7) and was the only cell line where ψ was outside an additive CI range. MIAPaCa-2 displayed additive interactions. Yao et al. have shown using FACS analysis that MIAPaCa-2 cells have the lowest proportion (0.03%) of side-population cells compared to other pancreatic cancer cells used: BxPC-3 (0.79%) and PANC-1 (7.75%) (39). Side-population cells share similarities to cancer stem cells (CSCs) and exhibit properties of pluripotential differentiation (both *in vivo* and *in vitro*) and higher levels of chemoresistance (39, 40). Qin et al. (41) evaluated interactions between 5-FU and Oxa based on the median-effect principle of Chou and Talalay (42) in human gastric cancer cell lines. Unlike the results described in Table III, which showed additivity or antagonism in pancreatic cancer cells, they found synergy. Interestingly, their results showed that the synergy was sequence dependent: simultaneous and sequential treatments of Oxa, followed by 5-FU produced synergistic interaction, with the opposite sequence yielding clear antagonism. Another study showed that synergistic interactions between 5-FU and Oxa were dependent on sequential exposure, with Oxa, followed by 5-FU, resulting in the most cytotoxic effect in multiple colorectal cancer cell lines [43]. Thus, a sequence-dependent

effect of Oxa and SN-38 may play an important role in addition to the drug weight ratio in achieving synergistic interactions between Oxa and SN-38 and better outcomes (41, 43). Simultaneous exposure of 5-FU and Oxa could explain the antagonistic interactions observed here (Table III).

The main novel finding of this study was that the triple combination of Oxa, 5-FU and SN-38 displayed antagonistic interactions in BxPC-3, PANC-1 (3D culture) and primary PIN-127 cells. PIN-127 cells showed strong antagonism, with a drug interaction term of 5.6. Patient-derived PDAC cell lines are a useful *in vitro* tool as they better reflect the heterogeneity of patient response to drug regimens, as seen in a recent report (44) where a panel of patient-derived PDAC cell lines exhibited differential sensitivity to FOLFIRINOX. It is important to note that additive DDIs can be highly beneficial clinically and that synergy is not a requirement for useful treatment regimens. While additivity is clinically useful, further evaluating the non-simultaneous use of the agents could potentially reduce toxicity, allowing access to this multi-drug regimen to more patients. The results shown here suggest that two-drug regimens such as Oxa and SN-38 could be equally effective and support the need for further preclinical *in vivo* studies.

Another interesting finding in PANC-1 was the shift from trending towards synergy in 2D towards antagonism in 3D. We describe this as trending towards antagonism as both conditions had confidence intervals that overlapped with additivity. Many studies suggest a molecular and phenotypic association between increased chemoresistance and the presence of an EMT-like phenotype of cancer cells (45–47). This suggests a hypothesis for the loss of synergy observed in the 3D growth of PANC-1, as Matrigel can modulate an EMT phenotype (48, 49). EMT involves a change in the extracellular matrix as cells detach from the basement membrane (BM) and engage the interstitial matrix (50, 51). Matrigel is a reconstituted BM isolated from Engelbreth-Holm-Swarm mouse sarcomas containing a complex mixture of macromolecules including laminin, type IV collagen and enactin that mimic BM *in vitro* (48). Puls et al. have also shown matrix-dependent PANC-1 cell sensitivity to gemcitabine, with increasing IC₅₀ values for cells grown in Matrigel (48). These observations are consistent with the hypothesis that extracellular matrix composition and tumour microenvironment are critical determinants of PDAC drug response and sensitivity (3, 4, 52).

The switch from synergy to antagonism observed in PANC-1 cells when grown in 3D compared to 2D could also result from reduced drug penetration into the centre of cell spheroids (53, 54). Cells grown in 3D may also be more secretory than their monolayer counterparts, potentially increasing paracrine signalling, resulting in differential drug responses. Spheroids face additional extracellular cues and physical conditions such as rigidity and limited adhesion,

which can affect drug response (55). Hypoxia, a common characteristic of pancreatic cancers, can alter tumour cell phenotype, which adapts their metabolism to sustain growth (56) and can result in genetic alterations, giving rise to multi-drug resistance (57). Spheroids such as those described in this study can have increased levels of hypoxia, which could explain the antagonistic switch observed (58).

The results shown here confirm that the agents of the FOLFIRINOX regimen can have various DDIs *in vitro* depending on the cell line tested. While the triple combination appeared antagonistic in many cell lines, meaning the net effect is less than the additive effect of individual agents, it still resulted in greater cell kill than any agent alone. Therefore, a better understanding of their pharmacodynamic interactions is warranted, particularly *in vivo*.

Early pharmacodynamic modelling of combination therapies (42) was successful in overcoming the assumptions and limitations implicit in the classical fractional inhibitory concentration index or checkerboard approach (59, 60). However, interaction parameters must be interpreted cautiously in that marginal values, although within objective definitions of synergy and antagonism, will not directly translate into clinically meaningful interactions.

This study was conducted *in vitro*, and the nature of interactions may differ *in vivo*. The results shown in this study demonstrated how LV enhancement of 5-FU was not statistically significant when carried out *in vitro* due to the lack of catabolic activity present in culture conditions. The use of *in vivo* PDX models could overcome this limitation and provide more evidence for the DDIs observed here. This study suggests the necessity of further investigation into the complex interactions among the FOLFIRINOX agents as a route to enhance their efficacy in pancreatic cancer.

Conclusion

Application of a mathematical model-estimated drug interaction parameter ψ reveals that pairwise and triple combinations of the FOLFIRINOX agents exert a range of pharmacodynamic drug-drug interactions across a panel of pancreatic cancer cell lines, with numerous combinations being antagonistic. Extension of this modelling analysis approach to *in vivo* models could provide greater insight into the optimisation of this first-line pancreatic cancer treatment regimen. Interestingly, analysis of the primary PDX-derived PIN-127 cell line showed antagonistic interactions among all drug combinations. These results suggest a complex interplay among the three agents that may be dependent upon specific tumour cell characteristics, and future work will use the PD data to assess whether lower concentrations and/or alternate schedules would be both efficacious and less toxic. This pharmacodynamic, model-informed approach provides

a quantitative platform to increase our understanding of complex drug interactions, with the objective of identifying a more efficacious and tolerable FOLFIRINOX regimen that would be feasible for a greater fraction of PDAC patients.

Supplementary Information The online version contains supplementary material available at <https://doi.org/10.1208/s12248-022-00752-8>.

Acknowledgements Graphical abstract was created with BioRender.com.

Author Contribution Taylor J Allen-Coyle – formal analysis, investigation and methodology, writing – original draft preparation.

Jin Niu – formal analysis, methodology.

Eva Welsch – formal analysis, investigation and methodology, writing – review.

Neil T. Conlon – formal analysis, writing – review and editing.

Weylon Garner – formal analysis, writing – early alternative draft preparation.

Martin Clynes – resources, supervision, writing – review and editing.

Finbarr O’Sullivan – resources, supervision, writing – review and editing.

Robert M. Straubinger – conceptualisation, resources, supervision, writing – review and editing.

Donald E. Mager – conceptualisation, resources, supervision, writing – review and editing.

Sandra Roche – conceptualisation, resources, supervision, writing – review and editing.

Funding This work was funded by Science Foundation Ireland (SFI), co-funded by the European Regional Development Fund (ERDF), Grant no.12/RC/2257/2.

This work was supported by research grants from the Pancreatic Cancer Research Fund UK (PCRF).

Declarations

Conflict of Interest The authors declare no competing interests.

Open Access This article is licensed under a Creative Commons Attribution 4.0 International License, which permits use, sharing, adaptation, distribution and reproduction in any medium or format, as long as you give appropriate credit to the original author(s) and the source, provide a link to the Creative Commons licence, and indicate if changes were made. The images or other third party material in this article are included in the article’s Creative Commons licence, unless indicated otherwise in a credit line to the material. If material is not included in the article’s Creative Commons licence and your intended use is not permitted by statutory regulation or exceeds the permitted use, you will need to obtain permission directly from the copyright holder. To view a copy of this licence, visit <http://creativecommons.org/licenses/by/4.0/>.

References

1. Siegel RL, Miller KD, Jemal A. Cancer statistics, 2020. *CA Cancer J Clin.* 2020;70(1):7–30. <https://doi.org/10.3322/caac.21590>.
2. Evans J, Chapple A, Salisbury H, Corrie P, Ziebland S. “It can’t be very important because it comes and goes” –patients’ accounts of intermittent symptoms preceding a pancreatic cancer diagnosis:

- a qualitative study. *BMJ Open*. 2014;4(2): e004215. <https://doi.org/10.1136/bmjopen-2013-004215>.
3. Adamska A, Elaskalani O, Emmanouilidi A, Kim M, Abdol Razak NB, Metharom P, et al. Molecular and cellular mechanisms of chemoresistance in pancreatic cancer. *Adv Biol Regul*. 2018;68:77–87. <https://doi.org/10.1016/j.jbior.2017.11.007>.
 4. Murakami T, Hiroshima Y, Matsuyama R, Homma Y, Hoffman RM, Endo I. Role of the tumor microenvironment in pancreatic cancer. *Ann Gastroenterol Surg*. 2019;3(2):130–7. <https://doi.org/10.1002/ags3.12225>.
 5. Andrén-Sandberg A. Pancreatic cancer: chemotherapy and radiotherapy. *N Am J Med Sci*. 2011;3(1):1–12. <https://doi.org/10.4297/najms.2011.31>.
 6. Conroy T, Desseigne F, Ychou M, Bouche O, Guimbaud R, Becouarn Y, et al. FOLFIRINOX versus gemcitabine for metastatic pancreatic cancer. *N Engl J Med*. 2011;364(19):1817–25. <https://doi.org/10.1056/NEJMoa1011923>.
 7. Vreeland TJ, McAllister F, Javadi S, Prakash LR, Fogelman DR, Ho L, et al. Benefit of gemcitabine/nab-paclitaxel rescue of patients with borderline resectable or locally advanced pancreatic adenocarcinoma after early failure of FOLFIRINOX. *Pancreas*. 2019;48(6):837–43. <https://doi.org/10.1097/MPA.0000000000001345>.
 8. Cavanna L, Stroppa EM, Citterio C, Mordenti P, Di Nunzio C, Peveri S, et al. Modified FOLFIRINOX for unresectable locally advanced/metastatic pancreatic cancer. A real-world comparison of an attenuated with a full dose in a single center experience. *Onco Targets Ther*. 2019;12:3077–85. <https://doi.org/10.2147/ott.s200754>.
 9. Yang F, Jin C, Fu DL, Warshaw AL. Modified FOLFIRINOX for resected pancreatic cancer: opportunities and challenges. *World J Gastroenterol*. 2019;25(23):2839–45. <https://doi.org/10.3748/wjg.v25.i23.2839>.
 10. Ueno H, Kosuge T. Adjuvant treatments for resectable pancreatic cancer. *J Hepatobiliary Pancreat Surg*. 2008;15(5):468–72. <https://doi.org/10.1007/s00534-008-1357-3>.
 11. Abbassi R, Algül H. Palliative chemotherapy in pancreatic cancer-treatment sequences. *Transl Gastroenterol Hepatol*. 2019;4:56. <https://doi.org/10.21037/tgh.2019.06.09>.
 12. Riedl JM, Posch F, Horvath L, Gantschnigg A, Renneberg F, Schwarzenbacher E, et al. Gemcitabine/nab-paclitaxel versus FOLFIRINOX for palliative first-line treatment of advanced pancreatic cancer: a propensity score analysis. *Eur J Cancer*. 2021;151:3–13. <https://doi.org/10.1016/j.ejca.2021.03.040>.
 13. Niu J, Straubinger RM, Mager DE. Pharmacodynamic drug-drug interactions. *Clin Pharmacol Ther*. 2019;105(6):1395–406. <https://doi.org/10.1002/cpt.1434>.
 14. Foucquier J, Guedj M. Analysis of drug combinations: current methodological landscape. *Pharmacol Res Perspect*. 2015;3(3): e00149. <https://doi.org/10.1002/prp2.149>.
 15. Molins EAG, Jusko WJ. Assessment of three-drug combination pharmacodynamic interactions in pancreatic cancer cells. *Aaps J*. 2018;20(5):80. <https://doi.org/10.1208/s12248-018-0235-4>.
 16. Mager DE, Jusko WJ. Development of translational pharmacokinetic-pharmacodynamic models. *Clin Pharmacol Ther*. 2008;83(6):909–12. <https://doi.org/10.1038/clpt.2008.52>.
 17. Zimmer A, Katzir I, Dekel E, Mayo AE, Alon U. Prediction of multidimensional drug dose responses based on measurements of drug pairs. *Proc Natl Acad Sci U S A*. 2016;113(37):10442–7. <https://doi.org/10.1073/pnas.1606301113>.
 18. Nelson SR, Zhang C, Roche S, O'Neill F, Swan N, Luo Y, et al. Modelling of pancreatic cancer biology: transcriptomic signature for 3D PDX-derived organoids and primary cell line organoid development. *Sci Rep*. 2020;10(1):2778. <https://doi.org/10.1038/s41598-020-59368-7>.
 19. Hou S, Tiriach H, Sridharan BP, Scampavia L, Madoux F, Seldin J, et al. Advanced development of primary pancreatic organoid tumor models for high-throughput phenotypic drug screening. *SLAS Discov*. 2018;23(6):574–84. <https://doi.org/10.1177/2472555218766842>.
 20. Ande A, Vaidya TR, Tran BN, Vicchiarelli M, Brown AN, Ait-Oudhia S. Utility of a Novel three-dimensional and dynamic (3DD) cell culture system for PK/PD studies: evaluation of a triple combination therapy at overcoming anti-HER2 Treatment resistance in breast cancer. *Front Pharmacol*. 2018;9:403. <https://doi.org/10.3389/fphar.2018.00403>.
 21. Roche S, O'Neill F, Murphy J, Swan N, Meiller J, Conlon NT, et al. Establishment and characterisation by expression microarray of patient-derived xenograft panel of human pancreatic adenocarcinoma patients. *Int J Mol Sci*. 2020;21(3). <https://doi.org/10.3390/ijms21030962>.
 22. Martin A, Clynes M. Comparison of 5 microplate colorimetric assays for in vitro cytotoxicity testing and cell proliferation assays. *Cytotechnology*. 1993;11(1):49–58. <https://doi.org/10.1007/bf00749057>.
 23. Y. Di Veroli G, Fornari C, Wang D, Mollard Sv, Bramhall JL, M. Richards F, et al. CombeneFit: an interactive platform for the analysis and visualisation of drug combinations. *Bioinformatics*. 2016;32 2866–8.
 24. Bliss CI. The toxicity of poisons applied jointly. *Annals of Applied Biology*1939. p. 585–615.
 25. Webb JL. Effect of more than one inhibitor. *Enzyme and Metabolic Inhibitors*1963. p. 66–79.
 26. Bruckner HW, Spigelman M. Leucovorin as a clinical potentiator of 5-fluorouracil toxicity and anticancer efficacy. *Mt Sinai J Med*. 1988;55(5):390–4.
 27. Showalter SL, Showalter TN, Witkiewicz A, Havens R, Kennedy EP, Hucl T, et al. Evaluating the drug-target relationship between thymidylate synthase expression and tumor response to 5-fluorouracil. Is it time to move forward? *Cancer Biol Ther*. 2008;7(7):986–94. <https://doi.org/10.4161/cbt.7.7.6181>.
 28. Harrison RL. Introduction to Monte Carlo simulation. *AIP Conf Proc*. 2010;1204:17–21. <https://doi.org/10.1063/1.3295638>.
 29. Chowbay B XJ, Wong JXG, Marvalim C, Ng SL, Sutiman N, Leong WF. Effects of oxaliplatin, capecitabine and irinotecan (OXIRI) on PDAC cell lines carrying different *Kras* mutational status ASCO annual meeting: *Journal of Clinical Oncology*; 2016.
 30. Kim Y, Han D, Min H, Jin J, Yi EC. Comparative proteomic profiling of pancreatic ductal adenocarcinoma cell lines. *Mol Cells*. 2014;37(12):888–98. <https://doi.org/10.14348/molcells.2014.0207>.
 31. Peters GJ, van Groeningen CJ, van der Wilt CL, Meijer S, Smid K, Laurensse E, et al. Time course of inhibition of thymidylate synthase in patients treated with fluorouracil and leucovorin. *Semin Oncol*. 1992;19(2 Suppl 3):26–35.
 32. Van der Wilt CL, Pinedo HM, Smid K, Peters GJ. Elevation of thymidylate synthase following 5-fluorouracil treatment is prevented by the addition of leucovorin in murine colon tumors. *Cancer Res*. 1992;52(18):4922–8.
 33. Tsujimoto H, Tsukioka S, Ono S, Sakamoto E, Sakamoto K, Tsuta K, et al. Effect of leucovorin on the antitumor efficacy of the 5-FU prodrug, tegafur-uracil, in human colorectal cancer xenografts with various expression levels of thymidylate synthase. *Oncol Lett*. 2010;1(6):973–80. <https://doi.org/10.3892/ol.2010.172>.
 34. Sakamoto E, Tsukioka S, Oie S, Kobunai T, Tsujimoto H, Sakamoto K, et al. Folylpolylglutamate synthase and gamma-glutamyl hydrolase regulate leucovorin-enhanced 5-fluorouracil anticancer activity. *Biochem Biophys Res Commun*. 2008;365(4):801–7. <https://doi.org/10.1016/j.bbrc.2007.11.043>.
 35. Nakamura A, Nakajima G, Okuyama R, Kuramochi H, Kondoh Y, Kanemura T, et al. Enhancement of 5-fluorouracil-induced

- cytotoxicity by leucovorin in 5-fluorouracil-resistant gastric cancer cells with upregulated expression of thymidylate synthase. *Gastric Cancer*. 2014;17(1):188–95. <https://doi.org/10.1007/s10120-013-0249-7>.
36. Zeghari-Squalli N, Raymond E, Cvitkovic E, Goldwasser F. Cellular pharmacology of the combination of the DNA topoisomerase I inhibitor SN-38 and the diaminocyclohexane platinum derivative oxaliplatin. *Clin Cancer Res*. 1999;5(5):1189–96.
 37. Lei F, Xi X, Rachagani S, Seshacharyulu P, Talmon GA, Pon-nusamy MP, et al. Nanoscale platform for delivery of active IRINOX to combat pancreatic cancer. *J Control Release*. 2021;330:1229–43. <https://doi.org/10.1016/j.jconrel.2020.11.029>.
 38. Deer EL, González-Hernández J, Coursen JD, Shea JE, Ngatia J, Scaife CL, et al. Phenotype and genotype of pancreatic cancer cell lines. *Pancreas*. 2010;39(4):425–35. <https://doi.org/10.1097/MPA.0b013e3181c15963>.
 39. Yao J, Cai HH, Wei JS, An Y, Ji ZL, Lu ZP, et al. Side population in the pancreatic cancer cell lines SW1990 and CFPAC-1 is enriched with cancer stem-like cells. *Oncol Rep*. 2010;23(5):1375–82. https://doi.org/10.3892/or_00000774.
 40. Rao CV, Mohammed A. New insights into pancreatic cancer stem cells. *World J Stem Cells*. 2015;7(3):547–55. <https://doi.org/10.4252/wjsc.v7.i3.547>.
 41. Qin B, Tanaka R, Shibata Y, Arita S, Ariyama H, Kusaba H, et al. In-vitro schedule-dependent interaction between oxaliplatin and 5-fluorouracil in human gastric cancer cell lines. *Anticancer Drugs*. 2006;17(4):445–53. <https://doi.org/10.1097/01.cad.0000198912.98442.cd>.
 42. Chou TC, Talalay P. Quantitative analysis of dose-effect relationships: the combined effects of multiple drugs or enzyme inhibitors. *Adv Enzyme Regul*. 1984;22:27–55.
 43. Failli A, Consolini R, Legitimo A, Orsini G, Romanini A, Spisni R, et al. Evaluation of in vitro cytotoxicity of oxaliplatin and 5-fluorouracil in human colon cancer cell lines: combination versus sequential exposure. *J Biol Regul Homeost Agents*. 2011;25(4):575–88.
 44. Begg SKS, Birnbaum DJ, Clark JW, Mino-Kenudson M, Wellner UF, Schilling O, et al. FOLFIRINOX. *Anticancer Res*. 2020;40(7):3659–67. <https://doi.org/10.21873/anticancer.14355>.
 45. Martinelli P, Carrillo-de Santa Pau E, Cox T, Sainz B, Jr., Dusetti N, Greenhalf W, et al. GATA6 regulates EMT and tumour dissemination, and is a marker of response to adjuvant chemotherapy in pancreatic cancer. *Gut*. 2017;66(9):1665–76. <https://doi.org/10.1136/gutjnl-2015-311256>.
 46. Quiñero F, Mesas C, Doello K, Cabeza L, Perazzoli G, Jimenez-Luna C, et al. The challenge of drug resistance in pancreatic ductal adenocarcinoma: a current overview. *Cancer Biol Med*. 2019;16(4):688–99. <https://doi.org/10.20892/j.issn.2095-3941.2019.0252>.
 47. Gaianigo N, Melisi D, Carbone C. EMT and treatment resistance in pancreatic cancer. *Cancers (Basel)*. 2017;9(9). <https://doi.org/10.3390/cancers9090122>.
 48. Puls TJ, Tan X, Whittington CF, Voytik-Harbin SL. 3D collagen fibrillar microstructure guides pancreatic cancer cell phenotype and serves as a critical design parameter for phenotypic models of EMT. *PLoS ONE*. 2017;12(11): e0188870. <https://doi.org/10.1371/journal.pone.0188870>.
 49. Shichi Y, Sasaki N, Michishita M, Hasegawa F, Matsuda Y, Arai T, et al. Enhanced morphological and functional differences of pancreatic cancer with epithelial or mesenchymal characteristics in 3D culture. *Sci Rep*. 2019;9(1):10871. <https://doi.org/10.1038/s41598-019-47416-w>.
 50. Lamouille S, Xu J, Derynck R. Molecular mechanisms of epithelial-mesenchymal transition. *Nat Rev Mol Cell Biol*. 2014;15(3):178–96. <https://doi.org/10.1038/nrm3758>.
 51. Walma DAC, Yamada KM. The extracellular matrix in development. *Development*. 2020;147(10). <https://doi.org/10.1242/dev.175596>.
 52. Shaked Y. The pro-tumorigenic host response to cancer therapies. *Nat Rev Cancer*. 2019. <https://doi.org/10.1038/s41568-019-0209-6>.
 53. Vinci M, Gowen S, Boxall F, Patterson L, Zimmermann M, Court W, et al. Advances in establishment and analysis of three-dimensional tumor spheroid-based functional assays for target validation and drug evaluation. *BMC Biol*. 2012;10:29. <https://doi.org/10.1186/1741-7007-10-29>.
 54. Al-Abd AM, Lee JH, Kim SY, Kun N, Kuh HJ. Novel application of multicellular layers culture for in situ evaluation of cytotoxicity and penetration of paclitaxel. *Cancer Sci*. 2008;99(2):423–31. <https://doi.org/10.1111/j.1349-7006.2007.00700.x>.
 55. Follin B, Juhl M, Cohen S, Pedersen AE, Kastrup J, Ekblond A. Increased paracrine immunomodulatory potential of mesenchymal stromal cells in three-dimensional culture. *Tissue Eng Part B Rev*. 2016;22(4):322–9. <https://doi.org/10.1089/ten.TEB.2015.0532>.
 56. Shah VM, Sheppard BC, Sears RC, Alani AW. Hypoxia: friend or foe for drug delivery in pancreatic cancer. *Cancer Lett*. 2020;492:63–70. <https://doi.org/10.1016/j.canlet.2020.07.041>.
 57. Erler JT, Cawthorne CJ, Williams KJ, Koritzinsky M, Wouters BG, Wilson C, et al. Hypoxia-mediated down-regulation of Bid and Bax in tumors occurs via hypoxia-inducible factor 1-dependent and -independent mechanisms and contributes to drug resistance. *Mol Cell Biol*. 2004;24(7):2875–89. <https://doi.org/10.1128/mcb.24.7.2875-2889.2004>.
 58. Riffle S, Hegde RS. Modeling tumor cell adaptations to hypoxia in multicellular tumor spheroids. *J Exp Clin Cancer Res*. 2017;36(1):102. <https://doi.org/10.1186/s13046-017-0570-9>.
 59. Odds FC. Synergy, antagonism, and what the chequerboard puts between them. *J Antimicrob Chemother*. 2003;52(1):1. <https://doi.org/10.1093/jac/dkg301>.
 60. Fratini F, Mancini S, Turchi B, Friscia E, Pistelli L, Giusti G, et al. A novel interpretation of the fractional inhibitory concentration index: the case *Origanum vulgare* L. and *Leptospermum scoparium* J. R. et G. Forst essential oils against *Staphylococcus aureus* strains. *Microbiol Res*. 2017;195:11–7. <https://doi.org/10.1016/j.micres.2016.11.005>.

Publisher's Note Springer Nature remains neutral with regard to jurisdictional claims in published maps and institutional affiliations.